Available online at www.sciencedirect.com
ScienceDirect

ELSEVIER

Renewable Energy 32 (2007) 532–546

RENEWABLE ENERGY

www.elsevier.com/locate/renene

Technical Note

A new multibody modelling methodology for wind turbine structures using a cardanic joint beam element

Xueyong Zhao[a,*], Peter Maißer[b], Jingyan Wu[c]

[a]*Eickhoff Maschinenfabrik GmbH, Hunscheidtstraße 176, 44789 Bochum, Germany*
[b]*Institute of Mechatronics at the Chemnitz University of Technology, Reichenhainer Str. 88, 09126 Chemnitz, Germany*
[c]*Institute of Thermodynamics, Department of Machinery of the Chemnitz University of Technology, Reichenhainer Str. 70, 09126 Chemnitz, Germany*

Received 21 March 2005; accepted 10 April 2006
Available online 7 July 2006

Abstract

This paper presents a new multibody modelling methodology for wind turbine structures. The methodology is based on the hybrid multibody system being composed of rigid, flexible bodies, force elements and joints. With a cardanic joint beam element based on the Timoshenko beam theory, the flexible bodies, e.g. rotor blades and tower, shafts, are modelled by a set of rigid bodies connected by cardanic joints geometrically and constrained by spring forces elastically, thus a whole wind turbine structure can be represented by a discrete system of rigid bodies, springs, and dampers. Using some concepts of the differential geometry, the Lagrange's motion equations of the multibody system are represented in explicit form. With this model, the global natural vibrations of a wind turbine structure of 600 kW are analysed.

Keywords: Wind turbine; Multibody system; Cardanic joint beam; Modal analysis

*Corresponding author. Tel.: +49 234 9752516; fax: +49 234 9752590.

0960-1481/$ - see front matter
doi:10.1016/j.renene.2006.04.010

Nomenclature

c_{ij}	stiffness
EI	bending stiffness
F_s	shear force
$f_{\underset{k}{l}}, f_{\underset{k}{m}}, f_{\underset{k}{\vartheta}}$	functions of the partitioning coefficient δ for the length, mass and inertia of the body k
GA_s	shear stiffness
g_{ab}	Riemannian metric
L	total length of a beam
$\underset{k}{l}$	lengths of the body k
$\underset{k}{K^i}$	applied force acting on body B_k
$k = 1, \ldots, K$	body number
M	total mass of a beam
M_b	bending moment
$M_k^{\ i}$	applied torque acting on bodyB_k
$\underset{k}{m}$	mass of body B_k
Q_a	generalised forces
q^a	representing point of MBS
R^n	configuration space
T	kinetic energy
V^n	Riemannian space
δ	partitioning coefficient
λ	constant
ϑ^{ij}	Binet's inertia tensor
$\underset{k}{\theta^{ij}} = \underset{k}{\vartheta^r_r}\,\delta^{ij} - \underset{k}{\vartheta^{ij}}$	ordinary inertia tensor of body B_k
$\underset{k}{\omega_i}$	angular velocity of body B_k
$\underset{j}{v_i}$	translational velocity of body B_k
Γ_{abc}	Christoffel symbol
∂_a	partial differential symbol

1. Introduction

1.1. Motivation

A wind power generator is a typical mechatronic system consisting of mechanical, electrical and control subsystems interacting among each other. The mechanical subsystem affects the electrical subsystem through the voltages in electrical machines, which are induced by mechanical movements, while the electrical subsystem influences the mechanical subsystem by electromagnetically produced forces and torques [1,2]. Both the effects are under the regulation of the control subsystem offering the potential to coordinate component functions and improve the performance of the wind power generator, such as fatigue life, stability, and power production.

For further improvements of the performance of wind power generators, a comprehensive models is essential. This model should have the following properties: firstly, it should capture the pertinent characteristics of the complete wind power generator as a low-degree of freedom system; secondly, it should be able to describe the electromechanical interaction of the mechanical and the electrical subsystems effectively; thirdly, it should be appropriate for controller design with the consideration of electromechanical characteristics; lastly, it should be suitable for time domain simulation. To fulfil these requirements, a discrete electromechanical system model is apparently essential.

Therefore, as the first step, a new multi-rigid-body model for the mechanical wind turbine structures will be developed.

1.2. Different concepts of the modelling

There are several possible methods to model the mechanical structure of a wind turbine: global Ritz-approach, finite element method, and multibody system (MBS) method.

Using the global Ritz-approach, the problem is solved by assuming that the shape of the deformed body with respect to a reference coordinate system can be approximated by a finite set of a specific class of shapes functions [3]. The shape functions are selected with respect to the geometric boundary conditions. The energy is integrated by time variations, so the motion equations are reduced to a ODE systems with respect to generalised coordinates. Finite element method is a local Ritz-approach, in which the elastic body is physically discretized into a number of regions connected by nodes [4]. The deformation of the elastic body with respect to a reference coordinate system is expressed in terms of shape functions, and the nodal degrees of freedom are associated with each region called an element. Both global Ritz-approach and finite element method require extremely high storage and long calculation time, especially for time-dependent systems, e.g. comprehensive wind power generator systems.

A MBS consists of rigid bodies interconnected by constraint elements and force elements. The constraint elements with different properties connecting the bodies constrain their motions [5–7]. Force elements like springs and dampers acting in discrete nodal points result in applied forces and torques acting on the bodies. A MBS possessing also flexibly bodies is called hybrid MBS being characterised by the interaction among rigid body movements and flexible deformations [8]. Its mechanics can be understood as a combination of rigid body dynamics and elastomechanics. For the systematic modelling and detailed analysis of a wind turbine structure, a hybrid MBS is more suitable, which can capture all the rigid and elastic mechanical components, couplings, important motions based on non-linear kinetics.

1.3. The current work

In this paper, a MBS model of wind turbines is presented. The wind turbine structure is idealised by replacing it with an assemblage of rigid and flexible bodies joined by force elements and constraints. The flexible components, e.g. tower, rotor blades and drive shaft, are discretized into many elastically connected rigid bodies by a cardanic joint beam element. The other components, e.g. hub, bed frame, gears, rotor of generator, are treated as rigid bodies. Based on the principle of virtual work, the Lagrange's motion equations of the MBS are generated in explicit form. With the established multibody model, the numerical analysis of the natural vibrations of a wind turbine structure of 600 kW is carried out.

2. Multibody system dynamics

The dynamics of a MBS could be considered as a point dynamics in the n-dimensional configuration space R^n of the MBS [5,6]. Introducing a metric (2-fold covariant tensor) in R^n defined by the kinetic energy of the MBS the R^n becomes a Riemannian space, denoted by V^n. Accordingly, all concepts and statements of the Riemannian geometry can be used to study the dynamics of MBS. The Riemannian geometry is the natural generalisation of the inner geometry of surface in the 3-dimensional Euclidean object space E^3.

For a holonomic MBS with kinematical tree structure having n degrees of freedom, the generalised coordinates q^a will be introduced according to the Denavit–Hartenberg notation:

$$q^a = s_a \underset{a}{\tau} + (1 - s_a) \underset{a}{\varphi}, \quad a = 1, \ldots, n, \tag{1}$$

where $\underset{a}{\tau}, \underset{a}{\varphi}$ denote complementary joint variables (displacement, angle) and $s_a = 1, 0$ describes the distribution of translational and rotational joints. $q = (q^a)$ is called the representing point of the MBS. The motion of a MBS can be understood as the motion of its representing points in the configuration space R^n. The motion equations of a MBS in R^n are Lagrange's equations of the second kind.

Starting from the kinetic energy of a holonomic scleronomic MBS:

$$T = \frac{1}{2} g_{ab}(q) \dot{q}^a \dot{q}^b, \tag{2}$$

the Lagrange's equations

$$(\dot{\partial}_a T)' - \partial_a T = Q_a \tag{3}$$

can be written explicitly as ODE system, which is linear with respect to the accelerations and quadratic with respect to the generalised velocities:

$$g_{ab}(q) \ddot{q}^b + \Gamma_{abc}(q) \dot{q}^b \dot{q}^c = Q_a. \tag{4}$$

The partial differentials are defined as $\dot{\partial}_a = (\partial/\partial \dot{q}_a)$, $\partial_a = (\partial/\partial q_a)$, $g_{ab} = \dot{\partial}_a \dot{\partial}_b T$ being symmetric, positive definite and non-singular defines a Riemannian metric in the n-dimensional configuration space R^n, R^n endowed with such a metric g_{ab} becomes a Riemannian space V^n. The Christoffel symbols of the first kind denote

$$\Gamma_{abc} = \frac{1}{2} (\partial_b g_{ac} + \partial_c g_{ab} - \partial_a g_{bc}), \tag{5}$$

which characterise—in the Newton-Euler mechanics—the coriolis —/centrifugal forces. Q_a denotes the covariant vector of the generalised forces of the MBS.

Introducing nonholonomic velocities (translational and angular velocities represented in a body-fixed frame) of the body B_k,

$$\underset{k}{v}_i = \underset{k}{u}_{ia}(q) \dot{q}^a, \underset{k}{\omega}_i = \underset{k}{\Omega}_{ia}(q) \dot{q}^a, \tag{6}$$

the generalised forces Q_a, the g_{ab} and the Christoffel symbols of the first kind Γ_{abc} can be represented as linear, quadratic and cubic forms, respectively, related to the so-called kinematic basic functions $\underset{k}{u}_{ia}, \underset{k}{\Omega}_{ia}$ of the MBS:

$$Q_a = \sum_{k=a}^{K} [\underset{k}{K}^i \underset{k}{u}_{ia} + (1 - s_a)\underset{k}{M}^i \underset{k}{\Omega}_{ia}], \tag{7}$$

$$g_{ab} = \sum_{k=b}^{K} [\underset{k}{m} \underset{k}{u}_{ia} \underset{k}{u}_{ib} + (1 - s_a)(1 - s_b)\underset{k}{\theta}^{ij} \underset{k}{\Omega}_{ia} \underset{k}{\Omega}_{jb}], \tag{8}$$

$$\Gamma_{abc} = (1 - s_b) \sum_{k=b}^{K} \varepsilon_i^{qr} [\underset{k}{m} \delta^{ij} \underset{k}{u}_{ja} \underset{k}{\Omega}_{qb} \underset{k}{u}_{rc} + (1 - s_a)(1 - s_c)\underset{k}{\vartheta}^{ij} \underset{k}{\Omega}_{ra} \underset{k}{\Omega}_{jb} \underset{k}{\Omega}_{qc}]. \tag{9}$$

3. Modelling of the wind turbine structures

3.1. Cardanic joint beam element

As shown in Fig. 1, the cardanic joint beam element consists of four coupled rigid bodies, which form a spatial joint rigid body system [9,10]. Every two adjacent bodies are connected by cardanic joints (body B_1 and B_2, body B_3 and B_4) or cylindrical joint (body B_2 and B_3) geometrically and physically. Totally, it has six degrees of freedom corresponding to four rotations, one torsion and one extension. The pure planar bending of the beam is calculated with the generalised coordinates of the two cardanic joints, the pure longitudinal distortion and pure torsion of the beam are represented by the movements of the cylindrical joint (combination of revolute and prismatic joints). Under the assumption of small deformations, the spatial motions of the joint beam can be described by the above-mentioned individual cases of their combination.

The inertial characteristics of the cardanic joint beam element are determined with respect to the undeformed position of the beam-continuum. The lengths $\underset{k}{l}$, the masses $\underset{k}{m}$, and moments of inertia $\underset{k}{\vartheta}_{ii}$ of the four bodies are defined by

$$\underset{k}{l} = \underset{k}{f}_l(\delta)L, \tag{10}$$

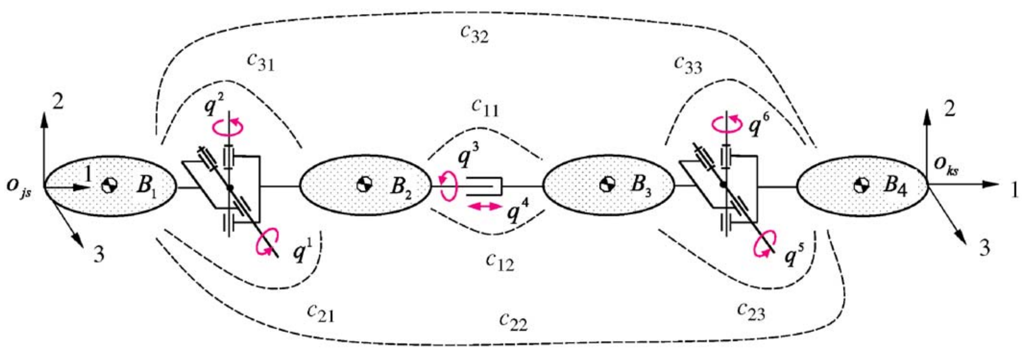

Fig. 1. Joint beam element.

$$\underset{k}{m} = \underset{k}{f}_m(\delta)M, \tag{11}$$

$$\underset{k}{\vartheta}_{ii} = \underset{k}{f}_\vartheta(\delta)\Theta_{ii}, \tag{12}$$

in which $k(=1,2,3,4)$ designates the number of the four bodies, and $i(=1,2,3)$ denotes one of the three axis of the body-fixed main inertial coordinate system. $\underset{k}{f}_l(\delta)$, $\underset{k}{f}_m(\delta)$, and $\underset{k}{f}_\vartheta(\delta)$ are functions of the partitioning coefficient $\delta(0<\delta<0.5)$. L and M denote the total length and the total mass of the continuum, and Θ_{ii} is the inertia of the beam-continuum.

The elastic characteristics of the cardanic joint beam element are determined by the physical couplings of the four rigid bodies. The physical couplings are represented by springs at the three joints and between the two terminal bodies. The spring constants $c_{ij}(i,j=1,2,3)$ marked by the dash lines in Fig. 1 define the force laws of the joint beam element, they are calculated by comparing the potential energy of the deformed elastic continuum with that of the joint beam element. Without the consideration of the shear deformation, the spring constants are calculated under the condition of an Euler–Bernoulli-beam [10]. However, if the geometric dimensions of the cross section of the continuum is not too small in comparison with the length, the shear deformation must be taken into account. Instead of the Euler-Bernoulli-beam model, the Timoshenko-beam model must be adopted [9], then the potential energy of the elastic continuum is written by

$$W = \frac{1}{2EI}\int M_b^2\,\mathrm{d}x + \frac{1}{2GA_s}\int F_s^2\,\mathrm{d}x, \tag{13}$$

where EI and GA_s are the bending rigidity and the effective shear rigidity of the continuum, M_b and F_s are the bending moment and shear force, respectively.

Defining

$$\lambda = \frac{GA_s L^2}{EI}, \tag{14}$$

the spring constants in the "$0-1-3$" bending plane are

$$c_{21} = c_{23} = \frac{6(1-2\delta)^2}{12+\lambda}\,GA_s L \tag{15}$$

and

$$c_{22} = \frac{12(\lambda\delta - \lambda\delta^2 + 1) - 2\lambda}{12+\lambda}\,\frac{EI}{L}. \tag{16}$$

Analogically, the spring constants in the "$0-1-2$" bending plane can also be obtained. The constant c_{11} of the torsional spring and c_{12} of the extensional spring are calculated respectively by

$$c_{11} = \frac{EA}{L}, \tag{17}$$

$$c_{12} = \frac{GI_t}{L}, \tag{18}$$

where EA and GI_t are the extensional rigidity and torsional rigidity of the continuum.

3.2. Treatment of the flexible components

Usually, the tower consists of a tubular steel construction with several conical sections and constant wall thickness in each section. Its characteristics are the axial symmetrical distributions of elasticity, moment of inertia and mass along the tower axis. The bending in the longitudinal direction (wind rotor axis direction) and lateral directions and the torsion are the predominant vibration modes, particularly, the lateral bending near the tower top corresponding to the second bending modes are substantially important, which can cause the lateral forces at the tower top and the gyroscopic forces of the wind rotor [2]. The torsion of the tower is also considered, because the torsion vibration can lead to high loads at the hub and the bed frame. The axial extension is not taken into account, because it has little influence on the dynamic behaviour of the complete wind turbine. Without the consideration of the rigidity and damping of foundation, the tower is treated as a variable sectioned thin walled beam attached to the ground with a fixed joint. Using three cardanic joint beam elements, the idealised beam is discretized into 12 elastically connected rigid bodies having 15 degrees of freedom.

The rotor blades of large wind turbines are usually made of glassfibre reinforced polyester or epoxy. From their roots to tips, the blade profiles change continuously. This leads to variable distributions of the masses, section moments of inertia, flexural rigidities about both centrelines, torsional rigidity about blade axes and pre-twist for optimal aerodynamic behaviours along the blade axes, by which the mechanical characteristics of the rotor blade are determined. Each of the blades undergoes flap bending, lag bending and elastic torsion. Because the blade is soft in the flap direction and relative rigid in the lag direction, the natural frequencies of the flap vibration are low, while the frequencies of the lag vibration are high. Since there exists an offset among the elastic axis, shear-centres axis and centres-of-mass axis, the flap bending, lag bending and torsion are coupled strongly, these dynamic characteristics play important roles in the vibrations of the entire wind turbine [2]. The axial extension is neglected, because its natural frequencies are very high, and consequently possesses weak influence on the dynamic behaviour of the entire wind power enerator.

With the cardanic joint beam element, the rotor blade is discretized. The number of necessary joint beam elements is selected according to the number of natural modes, which contribute to the description of the bending of the blades. This depends strongly on the blade construction and the exciting frequencies. For relatively rigid blades, the first and the second flap modes and the first lag modes are dominant in the vibrations of the wind rotor. Here, each blade is divided by two joint beam elements into eight rigid bodies with 10 degrees of freedom (or three joint beam elements with 12 rigid bodies and 15 dof.). The blade pre-twist is considered by the angle γ between the axes 3_{js} and 3_{ks} or 2_{js} and 2_{ks} of the two joint coordinate systems at the two terminal joint points o_{ks} and o_{js} of joint beam elements n and $n+1$, see Fig. 2.

Generally, the drive shaft is a short cone-formed hollow cylinder, through which the mechanical power and the large drive torque are transferred into the transmission. Using one joint beam element, it is divided into four rigid bodies. If the bending rigidity of the drive shaft is very large, the natural frequencies of its bending vibrations are far from the operation range of the wind turbine, then only the torsion vibration is considered. In this case, the drive shaft can be modelled by two rigid bodies connected with a torsional spring and a damper. The spring and damper constants are calculated based on its geometric dimensions and material constants.

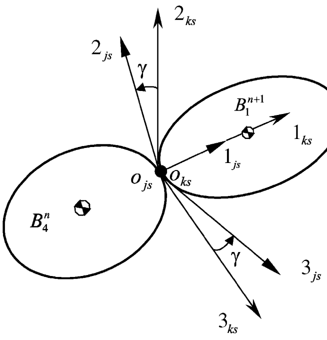

Fig. 2. Modelling of the blade pre-twist.

3.3. Treatment of rigid components

Nacelle and hub are formed mostly with cast iron. The nacelle acts as the machine carrier, which is coupled with the tower top by yaw mechanism. The hub connects the three rotor blades and the drive shaft. Through it, the large drive torque resulting from aerodynamic forces and the mass forces from the movement of the wind rotor are transferred into the drive shaft. Since only their masses and moments of inertia affect on the dynamic behaviour of the overall wind turbine system, the nacelle and hub are treated as rigid bodies.

In transmission, the gears are attached on the gearbox elastically and coupled with other gears by elastic contact forces. A multi-rigid-body system is very appropriate to describe the dynamic characteristics of the transmission, however, practically a model with flexible contacts and/or reactions is obviously not favourable for the complete modelling of the wind turbine, because such a model is highly non-linear, and thus causes much simulation expenditure. In order to reduce the degrees of freedom of the overall system, the gears are simplified as two or three equivalent masses.

The electromechanical properties of the asynchronous generator is simplified as a non-linear torsional damper fixed at one end with the high speed shaft and at another end with the electrical grid modelled as an infinite bus [11], the parameters of the non-linear damper can be obtained from the torque-slip relation ship in steady state of the asynchronous generator.

3.4. Description of couplings

The yaw mechanism, pitch mechanism and main bearing, as well as high-speed shaft can be regarded as geometric and physical couplings, which are described by joints and linear or non-linear force laws. The yaw mechanism connecting the tower top and the nacelle is simplified as an elastically constrained planar joint with two translations in the plane perpendicular to the tower axes and one rotation about the tower axes, the constraint forces at this joint are calculated by the force law of linear springs and dampers. The three blades are attached to the hub through pitch bearings, the pitch mechanism is represented by a cylindrical joint allowing the blade to rotate about its axis. The high-speed shaft connecting the gear transmission and the generator is modelled as a linear torsional spring and damper system.

4. Numerical simulation

4.1. Global natural modes

With the multibody model, the global natural vibrations of the mechanical structure of a wind turbine (see Table 1) are analysed systematically.

The most important dynamic properties of the complete systems are:

- the flap and lag vibrations of rotor blades,
- the first and second lateral and longitudinal vibrations of the tower,
- the torsional vibration of the drive train,
- the vibration interactions of the rotor blades and tower,
- the vibration interactions of the rotor blades and drive train.

For the convenience of description, the rotor blades are numbered and shown in Fig. 3. Fig. 4 shows the first lag modes of the three rotor blades. Each mode corresponds to three modes of the wind rotor, i.e. one collective mode and two differential modes.

In the collective mode shown in Fig. 4(a), all three blades vibrate with nearly the same phases and amplitudes. Their natural frequency is much higher than that of the lag vibration of an isolated rotor blade, because the inertial forces have the same orientation in the rotor plane about the rotor shaft, consequently, they lead to strong stiffening of a rotor blade in the lag direction. The collective modes, especially the first collective mode, are closely coupled with the torsion mode of the drive train. The inertial forces of the blades keep in equilibrium with the torsional moment of the drive train. If the natural frequencies of the collective lag vibration and torsional vibration are close, then coupled vibrations with large amplitudes will be excited. This can lead to the impairment of the operation or even to dangerous damage.

Figs. 4(b) and (c) present the two first differential lag modes. In Fig. 4(b), blades 2 and 3 vibrate in opposite directions, blade 1 whirls in the hub fixed coordinate system. In Fig. 4(c), blade 1 vibrates in opposite direction to the blades 2 and 3. Their frequencies are

Table 1
Parameters of a wind power generator

Type of wind turbine	Variable speed horizontal axis wind turbine
Nominal power	600 kW
Nominal wind speed	11.86 m/s
Nominal rotor speed	20–33 1/min
Radius of wind rotor	21.5 m
Tip speed ratio	6.25
Height of tower	52.2 m
Power control	Pitch
Cone angle	0°
Pre-twist of blades	16°
Tilt angle	5°
Mass of blade	ca. 2000 kg
Mass of hub	ca. 7500 kg
Mass of tower	ca. 60000 kg

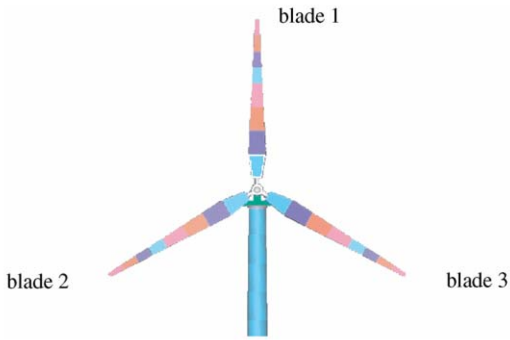

Fig. 3. Numeration of the three rotor blades.

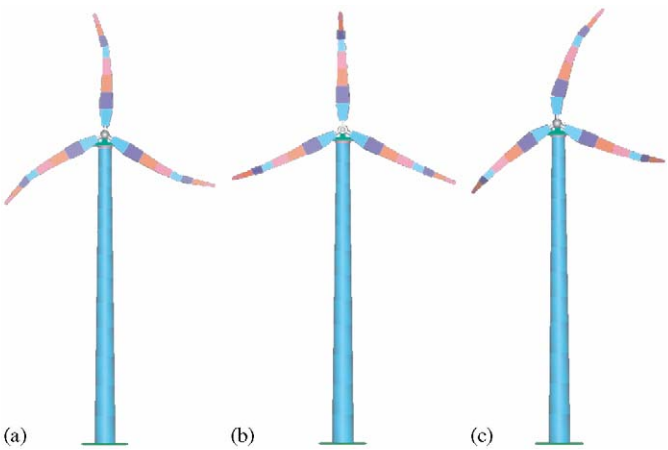

Fig. 4. First lag modes of the wind rotor: (a), collective lag mode, (b) and (c), differential lag modes.

close to the frequency of the isolated rotor blade. Since the inertial forces of the rotor blades do not keep in balance outside the rotor plane, the two first differential lag modes interact with the yaw mode and tilt mode of the wind rotor, respectively. But both of them have no coupling with the torsional mode of the drive train, because the inertial forces are in equilibrium in the rotor plane about the drive shaft.

Similarly, the first flap modes of the blades also lead to three modes of the wind rotor, one of which is collective and two are differential. In the collective flap mode, see Fig. 5(a), the three blades have identical amplitudes and phases, they interact with the first longitudinal mode of the tower. The differential mode in Fig. 5(b), in which the blades 2 and 3 vibrate in opposite directions, is coupled with the yaw mode of the wind rotor, while the differential mode shown in Fig. 5(c), in which blades 2 and 3 vibrate in the same direction and in the opposite direction to blade 1, is coupled with the tilt mode of the wind rotor.

With consideration of the rotor speed (operation state), the combination of the yaw and tilt vibrations leads to the whirling of the wind rotor due to the inertial and gyroscopic forces. The orientation of the drive shaft changes spatially and a shaft-axis-fixed point

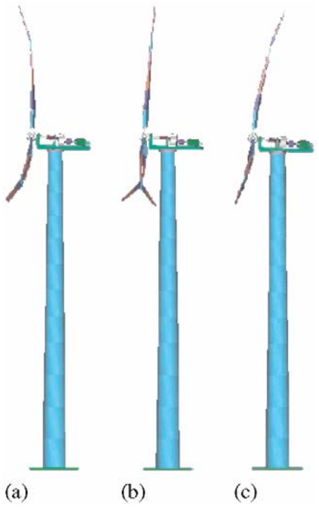

Fig. 5. First flap modes of the wind rotor: (a) collective flap mode, (b) and (c) differential flap modes.

moves along an ellipse. If the ellipse is followed by the point in the same direction of the rotation of the drive shaft, this is called forward whirling, otherwise it is called backward whirling. The natural frequencies of the whirlings depend on the angular rotor speed. With the increase of the angular rotor speed, the natural frequency of the forward whirling increases, while the natural frequency of backward whirling reduces. If the natural frequencies of the differential lag vibrations and the whirling of the wind rotor are very close, the whirling will take place.

In still state, there are no centrifugal and gyroscopic forces resulting from the rotary speed of the wind rotor, the vibration characteristics are affected only by the inertial forces and the elastic forces, hence, the global natural vibrations in still state differ from that in operating states. Here, as an example, the longitudinal vibration of the tower in the two states is discussed in order to interpret the difference of the natural vibrations in the two states. Fig. 6(a) shows the over-dazzled pictures of the fist longitudinal vibration of the tower in the still state, which is coupled only with the collective flap mode of the wind rotor. In this case, the rotor plane experiences only tilt motion and translation in the longitudinal direction, but no lateral movement and yaw movement. However, in operation state, the vibrations shown in Fig. 6(b) affect mutually because of the complicated mechanism of the vibration couplings, as described in Fig. 7. When the tower vibrates in the longitudinal direction, the rotating wind rotor disk tilts, then the gyroscopic force develops, which drives the wind rotor to yaw and to vibrate in the lateral direction, further, blades 2 and 3 vibrate in the flap direction with opposite phases, which influence the tower vibrations again. In this case, the tower vibrates simultaneously in lateral and longitudinal directions.

4.2. Natural frequencies

Under the angular rotor speed, the vibration characteristics are affected by centrifugal, gyroscopic, inertial and inner elastic forces. Some natural frequencies vary substantially with

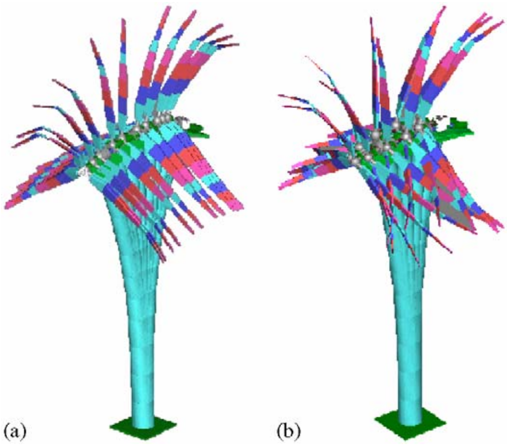

Fig. 6. Comparison of the coupled longitudinal vibration of tower and flap vibration of blades in still state and in operation state.

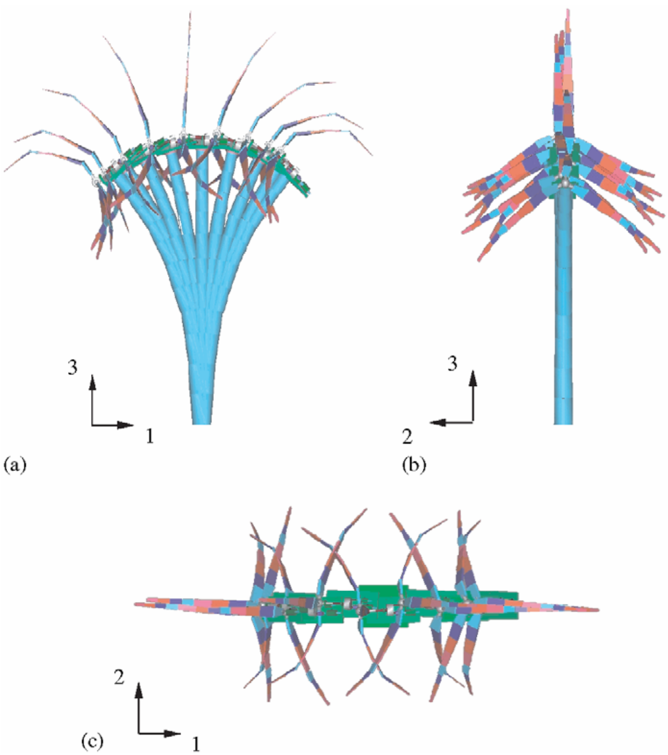

Fig. 7. Coupled longitudinal vibration of tower and lap vibration of blades in operation state.

the angular rotor speed, because of the effects of these dynamic forces. Figs. 8(a) and (b) show the natural frequencies of the lateral and longitudinal vibrations of the tower, and Figs. 8(c) and (d) present the natural frequencies of the yaw and the tilt vibration of the wind rotor.

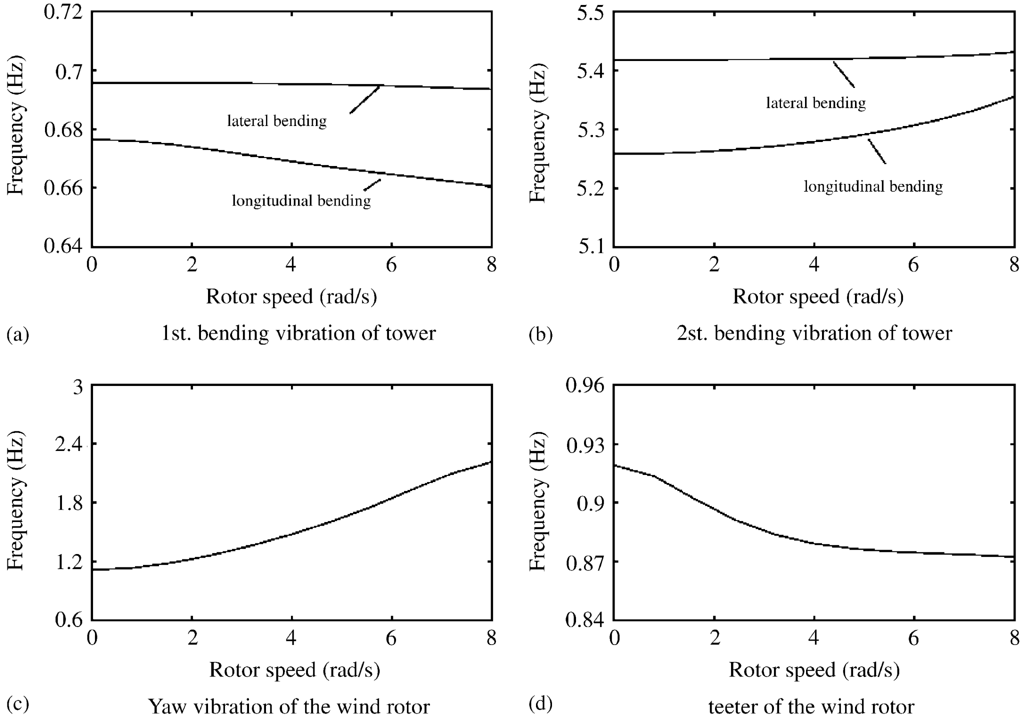

Fig. 8. Frequencies of the tower and nacelle with the angular rotor speed.

The frequencies of the first and second lateral vibration change very little with the increase of the angular rotor speed. In the lateral vibrations of the tower, the wind rotor translates in the lateral direction, the orientation of the drive shaft hardly ever changes, the gyroscopic effect of the wind rotor is very weak, thus the natural frequencies of the lateral vibrations are not greatly affected by the angular rotor speed. However, the natural frequency of the first longitudinal vibration is sensitive to the angular rotor speed, because the longitudinal vibration causes vibration couplings of yaw and tilt of the wind rotor, and lateral vibration of the tower, flap vibration of rotor blades, inversely, the gyroscopic force caused by the yaw movement drives the longitudinal vibration again. As a result, this leads to the frequency decrease of the coupled longitudinal vibration of the tower with increase of the angular rotor speed.

In Fig. 8(b), the natural frequency of the second longitudinal vibration increases with the angular rotor speed, because the second longitudinal vibration of the tower drives the wind rotor disk to tilt, at high angular rotor speeds, the inertial and centrifugal forces in the rotor plane are very large, they prevent the wind rotor disk from tilting.

In still state, the yaw and the tilt vibration do not interact on each other, but in operation state, the yaw vibration is coupled strongly with the tilt vibration because of the gyroscopic forces. In Figs. 8(c) and (d), the frequency of the yaw vibration increases with the angular rotor speed, but the frequency of the tilt vibration decreases. If the natural frequency of the lag vibration of the rotor blades are close to the natural frequencies of the yaw vibration and the tilt vibration, the global whirling of the wind rotor could be caused consequently.

Figs. 9(a) and (b) present the frequencies of the first and the second flap vibrations of the wind rotor. All three frequencies of the first flap vibrations increase with the angular rotor speed, and they are larger than the frequencies of the isolated blade, because of the stiffening from the inertial and centrifugal forces. The frequency of the first collective flap vibration is smaller than the natural frequencies of the two first differential flap vibrations, because the differential flap vibrations are coupled with the tilt and the yaw vibration of the wind rotor, and therefore a reinforcement takes place because of the inertial forces.

Figs. 9(c) and (d) show the first and the second natural frequencies of the lag vibrations of the wind rotor. Because of the centrifugal forces the lag frequencies increase with the angular rotor speed, but not obviously. The natural frequencies of the collective lag vibrations are much higher than that of the differential vibration, because the collective lag vibrations cause collective inertial forces in the rotor plane. The collective inertial forces through the hub prevent the lag vibrations. The natural frequencies of the two differential lag vibrations are close and a little higher than that of the frequencies of the isolated blade.

The line of $1p$ in the Fig. 9 marks the basic harmonious vibration with a frequency corresponding to the angular rotor speed. The lines $2p$ and $3p$ represent higher harmonious vibrations. The harmonious vibration by wind turbines can be caused by imbalance in rotor blades and by the tower shade. For a stationary operation, the rotor speed should lie

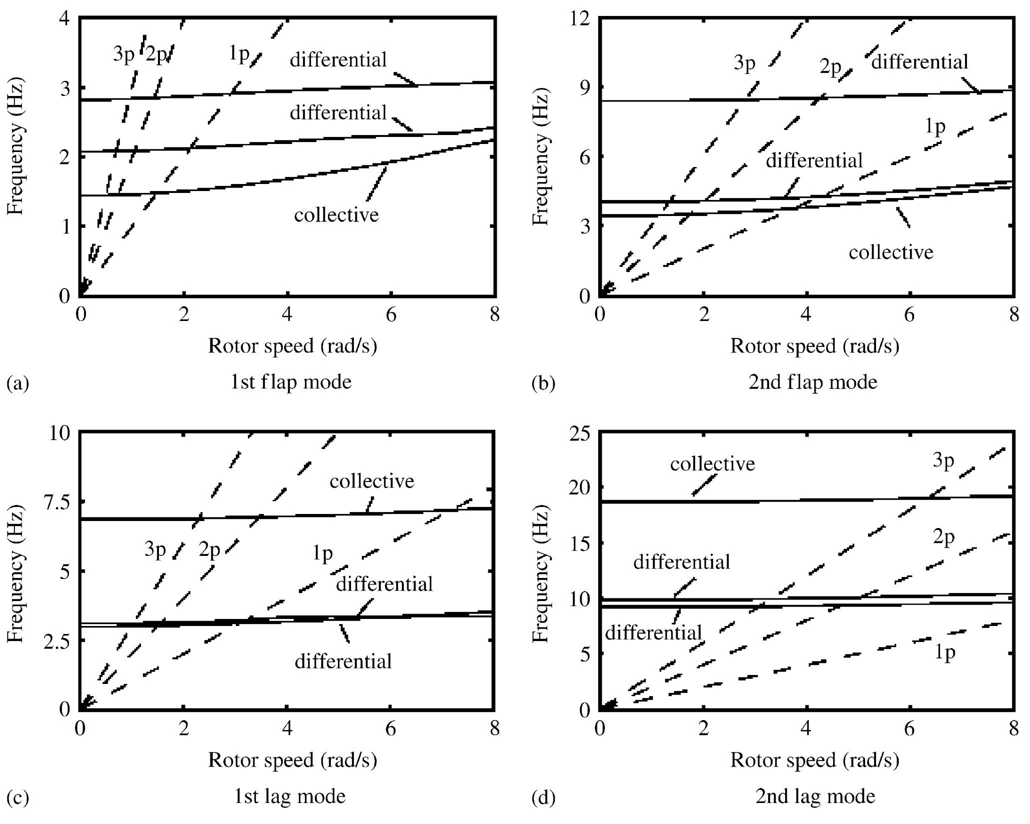

Fig. 9. Frequencies of the rotor blades with the angular rotor speed.

in a sufficient distance from the intersections of the harmonious vibration lines and the curve of the natural frequencies to avoid the resonant vibration.

5. Conclusion

A new MBS methodology has been presented for modelling the mechanical subsystem of a horizontal axis wind power generator. On the basis of the cardanic joint beam element, the complete flexible wind turbine structure is divided into a multi-rigid-body system consisting of rigid bodies, springs, dampers and constraint joints. With it almost all pertinent dynamic characteristics of the wind turbine are captured with a low degree of freedom model. This methodology is suitable for the analysis of global vibrations, dynamic loads, and is appropriate for the time-domain simulation.

This work will be extended in later papers to a discrete electromechanical MBS for complete wind power generators based on the principle of virtual work. The mechanical and electrical subsystems can be unified in Lagrange's equations of the second kind.

References

[1] Zhao X, Maißer P. A novel power splitting drive train for variable speed wind power generators. Int J Renew Energy 2003;28:2001–11.
[2] Zhao X. Simulation des dynamischen Verhaltens einer Windenergieanlage als mechatronisches System. Germany: Shaker Verlag GmbH; 2004.
[3] Baumgart A, Meywerk M. Ein mathematisches Modell für Windkraftanlagen. ZAMM 1999;79:281–2.
[4] Horvath G, Toth L. A wind turbine tower analysis with finite element method. DEWEK 2000. Tagungsband 2000:299–302.
[5] Maißer P. Analytische Dynamik von Mehrkörpersystemen. ZAMM 1988;68:463–81.
[6] Maißer P. A differential-geometric approach to the multibody system dynamics. ZAMM 1991;71:116–9.
[7] Schiehlen W. Advanced multibody system dynamics—simulation and software tools. London: Kluwer Academic Publishers; 1993.
[8] Schwertassek R, Wallrapp O. Dynamik flexibler Mehrkörpersysteme. Braunschweig: Vieweg Verlag; 1999.
[9] Zhao X, Maißer P, Freudenberg H. A cardanic joint beam element for the rotor blades of wind turbines. Institute of Mechatronics at the Chemnitz University of Technology; 2001.
[10] Rauh, J. Ein Beitrag zur Modellierung elastischer Balkensysteme. VDI, Reihe 18, Nr. 37, Duesseldorf; 1987.
[11] Heier, S. Windkraftanlagen im Netzbetrieb. 2. Auflage, B.G. Teubner Stuttgart;1995.